# LST Calculator: A Python Tool for Retrieving Land Surface Temperature from Landsat 8 Imagery

**Chapter** · January 2016



**1 author:**

Hakan Oguz
Kahramanmaras Sutcu Imam University

# Environmental Sustainability and Landscape Management

***Editors***

Recep Efe

İsa Cürebal

Abdalla Gad

Brigitta Tóth

**St. Kliment Ohridski University Press, Sofia**

# Environmental Sustainability and Landscape Management

**Editors**

Recep Efe
İsa Cürebal
Abdalla Gad
Brigitta Tóth

ISBN 978-954-07-4140-6

ST. KLIMENT OHRIDSKI UNIVERSITY PRESS
SOFIA, 2016

**Editors**

**Prof. Dr. Recep Efe**
Balikesir University,
Faculty of Arts and Sciences
Department of Geography
Balıkesir, Turkey

**Prof. Dr. Isa Cürebal**
Balikesir University
Faculty of Arts and Sciences
Department of Geography
Balıkesir, Turkey

**Prof. Dr. Abdalla Gad**
Environmental Studies and Land Use Division,
National Authority for Remote Sensing and Space Sciences (NARSS),
Cairo, Egypt

**Prof. Dr. Brigitta Tóth**
University of Debrecen
Faculty of Agricultural and Food Sciences and Environmental Management
Debrecen, Hungary

St. Kliment Ohridski University Press

ISBN 978-954-07-4140-6

The contents of chapters/papers are the sole responsibility of the authors, and publication shall not imply the concurrence of the Editors or Publisher.



Cover Design: İsa Cürebal

# CONTENTS

# Chapter 36

# LST Calculator: A Python Tool for Retrieving Land Surface Temperature from Landsat 8 Imagery

Hakan OĞUZ*

## INTRODUCTION

Land surface temperature (LST) is a key parameter which plays an important role in many environmental studies (Xiao *et al.,* 2007). Urban heat island effect, global warming, enhanced green-house effects and other environmental problems have become crucial subjects to overcome in the last decades. LST retrieval using remotely sensed data is currently one of the most popular subjects in environmental studies during the last couple of decades with Landsat data.

Several algorithms have been developed by researchers to calculate LST but the most used ones are Split-Window (SW) algorithm, Single-Channel (SC) algorithm, and Radiative Transfer Equation (RTE) (Abrams, 2000; Cristóbal, Jiménez-Muñoz, Sobrino, Ninyerola, & Pons, 2009; Jimenez-Munoz, Sobrino, Skokovic, Mattar, & Cristobal, 2014; Jimenez-Munoz & Sobrino, 2003; Oguz, 2013; Oguz, 2015; Yu, Guo, & Wu, 2014; Sobrino *et al.,* 2007).

In this study, the radiative transfer equation-based method was employed due to the fact that it is easy to implement and it was also found to have the highest accuracy compared to SW and SC algorithms (Yu *et al.,* 2014). Landsat 8 data contains 11 bands ranging from 15m panchromatic to 100m thermal bands. Landsat 8 bands 4 (Red), 5 (NIR), and 10 (TIR-1) are the only bands required by the toolbox to calculate LST.

## MATERIALS AND METHODS

### Landsat 8 TIRS Bands

Landsat 8 satellite was launched in February 2013 for the continuity of remote sensing data at high spatial resolution in the Landsat Data Continuity Mission. Landsat 8 carries two instruments: The operational Land Imager (OLI) sensor along with multispectral bands 1-7 and 9 with 30 meters (except for band 8 which is panchromatic with 15m resolution) and the Thermal Infrared Sensor (TIRS) which collects data at a 100m spatial resolution with two bands (bands 10 and 11). Landsat 8 products are delivered as 16-bit images which enable better characterization of land cover state and condition.

The new TIRS have an advancement over the previous TM/ETM sensors by having two TIR bands in the atmospheric window between 10 and 12 µm (Jimenez-Munoz *et al.,* 2014). As illustrated in Figure 1 below, the previous single band has been split into two TIR bands which are now narrower than the previous TM/ETM TIR band. Further information regarding the sensor is presented in Table 1.

---

* Assoc. Prof. Dr., Kahramanmaras Sutcu Imam University, Faculty of Forestry, Dept. of Landscape Architecture, hakan@ksu.edu.tr

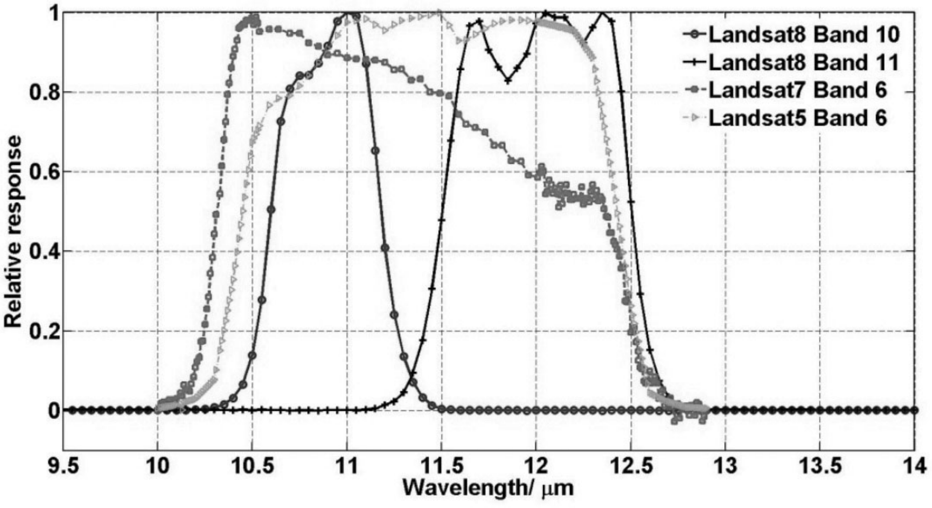


**Figure 1:** Spectral Response for thermal bands of different sensors (Source: Yu *et al.,* 2014)

**Table 1:** Characteristics of the Landsat 8 Data

| **Band No** | **Band Name** | **Band Width(μm)** | **Spatial Resolution (m)** |
|---|---|---|---|
| Band 1 | Coastal/Aerosol | 0.435 - 0.451 | 30 |
| Band 2 | Blue | 0.452 - 0.512 | 30 |
| Band 3 | Green | 0.533 - 0.590 | 30 |
| Band 4 | Red | 0.636 - 0.673 | 30 |
| Band 5 | NIR | 0.851 - 0.879 | 30 |
| Band 6 | SWIR-1 | 1.566 - 1.651 | 30 |
| Band 7 | SWIR-2 | 2.107 - 2.294 | 30 |
| Band 8 | Pan | 0.503 - 0.676 | 15 |
| Band 9 | Cirrus | 1.363 - 1.384 | 30 |
| Band 10 | TIR-1 | 10.60 - 11.19 | 100 |
| Band 11 | TIR-2 | 11.50 - 12.51 | 100 |

(Source: Landsat 8 Data Users Handbook, 2016)

### The Radiative Transfer Equation (RTE) Algorithm

The RTE algorithm retrieves LST ($T_S$) using the equation (1):

$$T_s = \left[ \frac{c_2}{\lambda \ ln \left\{ \frac{c_1}{\lambda^5 \left[ \frac{L_{sen} - L_u - \tau(1-\varepsilon)L_d}{\tau\varepsilon} \right]} + 1 \right\}} \right] \qquad (1)$$

where $T_s$ is the land surface temperature, ε is the land surface emissivity, $L_u$ is the up-welling atmospheric radiance, $L_d$ is the down-welling atmospheric radiance, $\tau$ is the atmospheric transmissivity, $\lambda$ is the effective band wavelength, $c_1 = 1.19104x10^8 W\mu m^4 m^{-2} sr^{-1}$ and $c_2 = 14387.7\ \mu m\, K$ are the constants. $L_{sen}$ is the thermal radiance at-sensor level and calculated by as follows:

$$L_{sen} = [\varepsilon B_{TS} + (1 - \varepsilon)L_d]\tau + L_u \quad (2)$$

where $B_{TS}$ is the spectral radiance (W/(m2 sr μm)).

The RTE method was selected and used in this particular study due to the fact that not only the model requires minimal and more accessible input data but also the procedure was found to be the least bias compare to other methods according to Yu *et al.,* (2014).

**NDVI retrieval**

Normalized difference vegetation index (NDVI) is a simple numerical index to assess the presence of live green vegetation. For Landsat 8 imagery, NDVI is computed using band 4 (RED) and band 5 (NIR) with the following Eq. 3:

$$NDVI = \frac{\rho_{band5} - \rho_{band4}}{\rho_{band5} + \rho_{band4}} \quad (3)$$

where $\rho_{band5}$ stands for the spectral reflectance measurements acquired in the NIR band and $\rho_{band4}$ represents the spectral reflectance measurements acquired in the RED band.

Afterwards, this NDVI file is used as an input to calculate Fractional Vegetation Cover (FVC) values as shown in Eq. 4 below (Skokovic *et al.,* 2014):

$$FVC = \frac{NDVI - NDVI_s}{NDVI_v + NDVI_s} \quad (4)$$

where $NDVI_v$ and $NDVI_s$ stand for NDVI values of full vegetation cover and bare soil respectively.

**Emissivity retrieval**

Emissivity is described as a proportionality factor, which scales black body radiance by Jimenez-Munoz, Sobrino, Gillespie, Sabol, & Gustafson (2006) to estimate emitted radiance. Therefore, emissivity is a vital role for the accuracy of land surface temperature retrieval. Several approaches have been proposed over the past decades to retrieve land surface emissivity from NDVI (Jimenez-Munoz *et al.,* 2006; Sobrino & Raissouni, 2000; Valor & Caselles, 1996; Van de Griend & Owe, 1993). In this study, Sobrino *et al.*'s (2008) land surface emissivity retrieval approach has been adopted (Eq. 5):

If $FVC = 0$ → $\varepsilon = 0.979 - 0.046 * \rho_{band4}$ (5a)

If $0 < FVC < 1$ → $\varepsilon = 0.971(1 - FVC) + 0.987 * FVC$ (5b)

If $FVC = 1$ → $\varepsilon = 0.99$ (5c) where FVC stands for Fractional Vegetation Cover, $\varepsilon$ stands for land surface emissivity, and $\rho_{band4}$ represents spectral reflectance for the RED band (band 4) of Landsat 8.

Any of the two thermal bands of Landsat 8 can be used in this study but Jimenez-Munoz et al. (2014) recommends Landsat 8 band 10 (TIR-1) due to its high atmospheric transmissivity. Therefore, band 10 has been employed in this study for the LST retrieval.

## RESULTS

### A Python Tool: LST Calculator

This program was developed using Python programming language (Python 2.7) and it can be run within ArcGIS Desktop, ESRI's complete GIS mapping platform. A request to get the tool can be made by contacting the author through his personal webpage at https://hakanoguz.wordpress.com. This toolbox consists of seven individual tools as illustrated in Figure 2 below: 1- TOA Radiance, 2- TOA Reflectance, 3- NDVI, 4- FVC, 5- Emissivity, 6- Lsen and 7- LST. The general flow diagram of the tool is given in Figure 3.

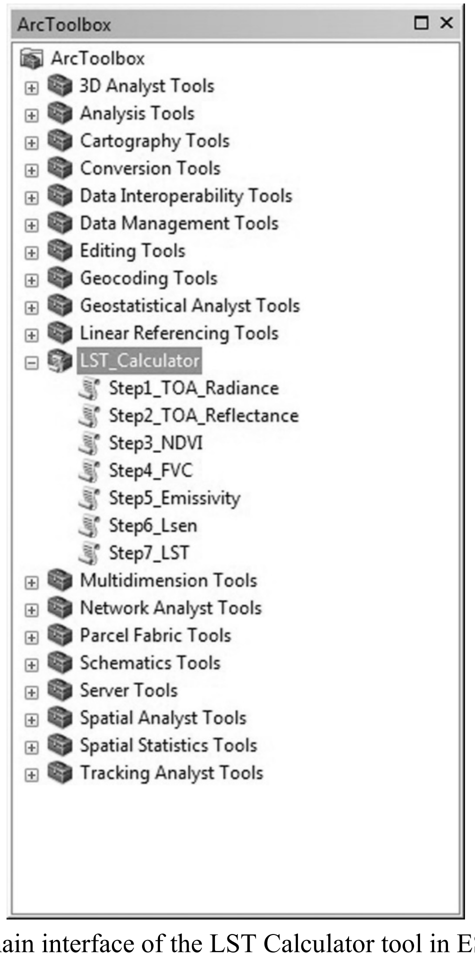


**Figure 2:** The main interface of the LST Calculator tool in ESRI ArcToolbox

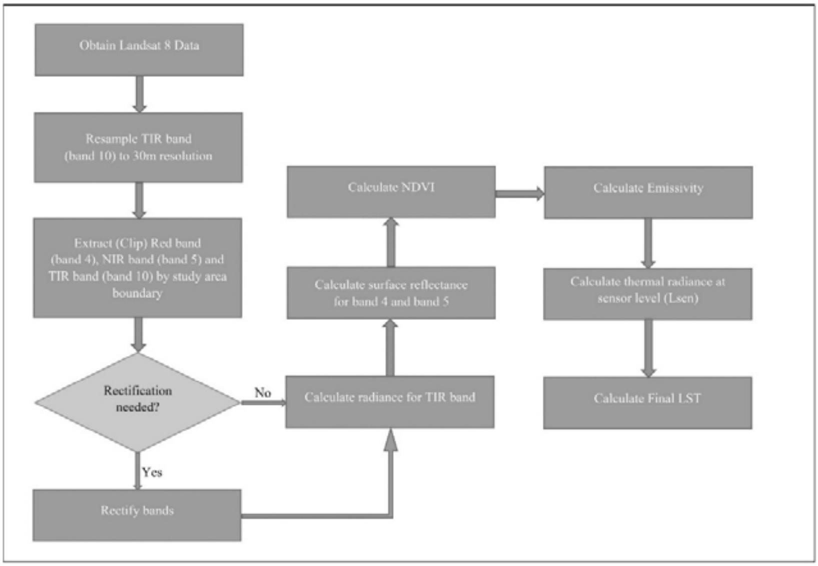


**Figure 3:** The flow diagram of the LST Calculator toolbox

**TOA Radiance**

At sensor Radiances for Landsat 8 bands are computed from following Eq. 6 (LDUH, 2016):

$$L_\lambda = (M_L * Q_{cal}) + A_L \tag{6}$$

where $L_\lambda$ is spectral radiance ($W/(M^2 * sr * \mu m)$), $M_L$ represents radiance multiplicative scaling factor for the band, $A_L$ is the radiance additive scaling factor for the band, and $Q_{cal}$ is pixel value in DN. These values are obtained from the metadata. Furthermore, Figure 4 illustrates the radiance calculation interface of the software tool.

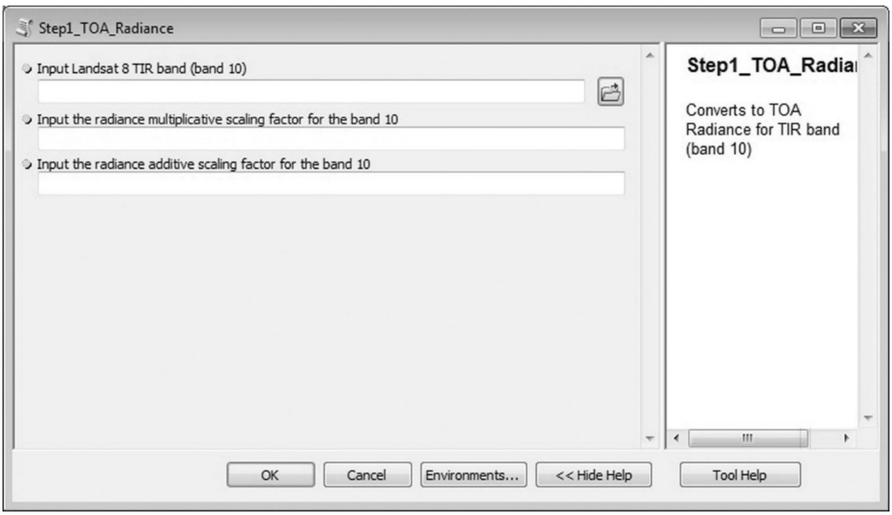


**Figure 4:** Radiance calculation interface for the TIR band

**TOA Reflectance**

After calculating at sensor radiances, planetary reflectances for the Landsat 8 RED and NIR bands (band 4 and band 5 only) are computed using the Eq. 7 (LDUH, 2016):

$$\rho_\lambda = \frac{M_p * Q_{cal} + A_p}{sin(\theta)} \tag{7}$$

where $\rho_\lambda$ is unitless TOA planetary reflectance, $M_p$ is reflectance multiplicative scaling factor for the band, $Q_{cal}$ is pixel value in DN, $A_p$ is reflectance additive scaling factor for the band, and $\theta$ is solar elevation angle.

Figure 5 below shows the planetary reflectance calculation interface of the program. This step requires four parameters: Landsat 8 RED or NIR band, reflectance multiplicative scaling factor, reflectance additive scaling factor, and solar elevation angle,

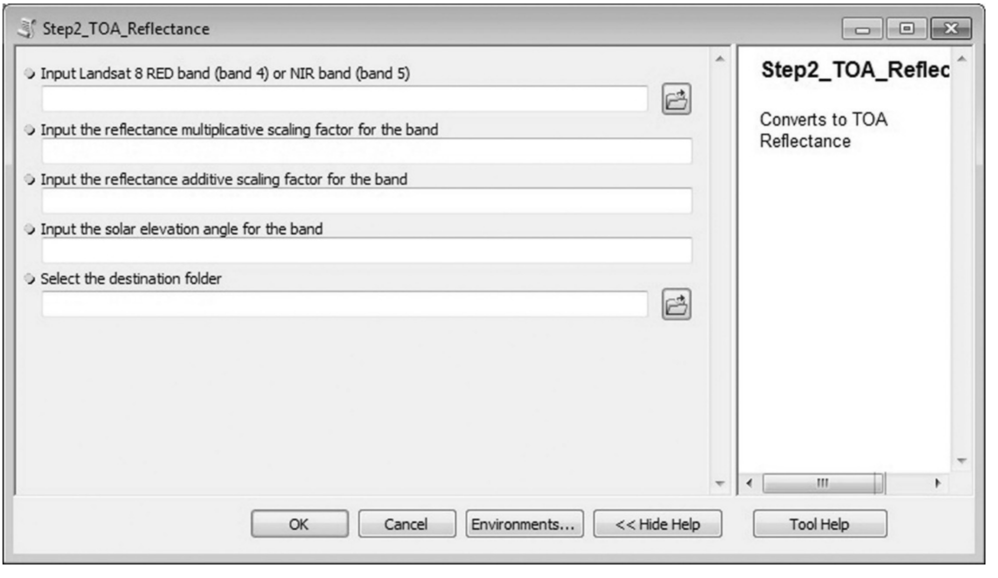


**Figure 5**: Reflectance calculation interface

NDVI interface of the tool is illustrated in Figure 6 below. This step requires RED band reflectance file and NIR band reflectance file only.

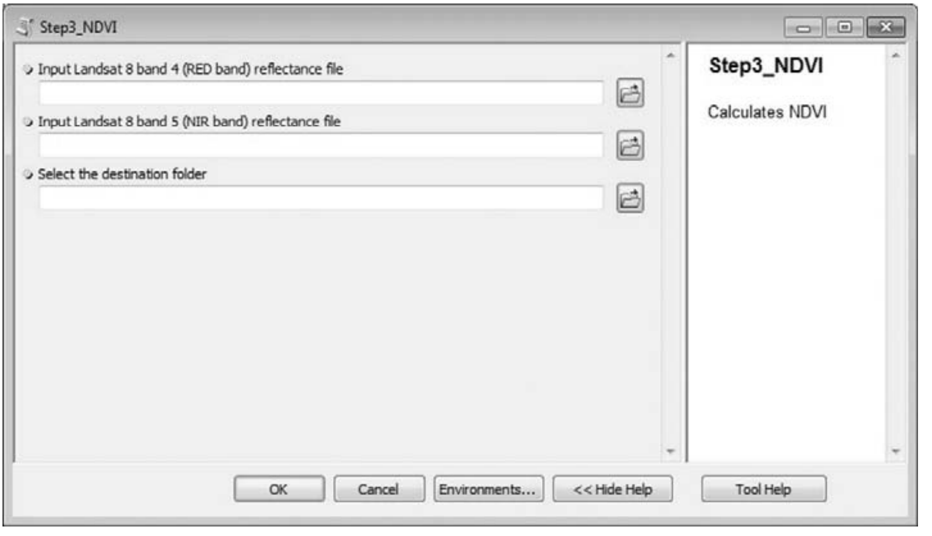


**Figure 6:** NDVI calculation interface

The FVC calculation interface is shown in Figure 7 below. In this step, the only band required is NDVI file.

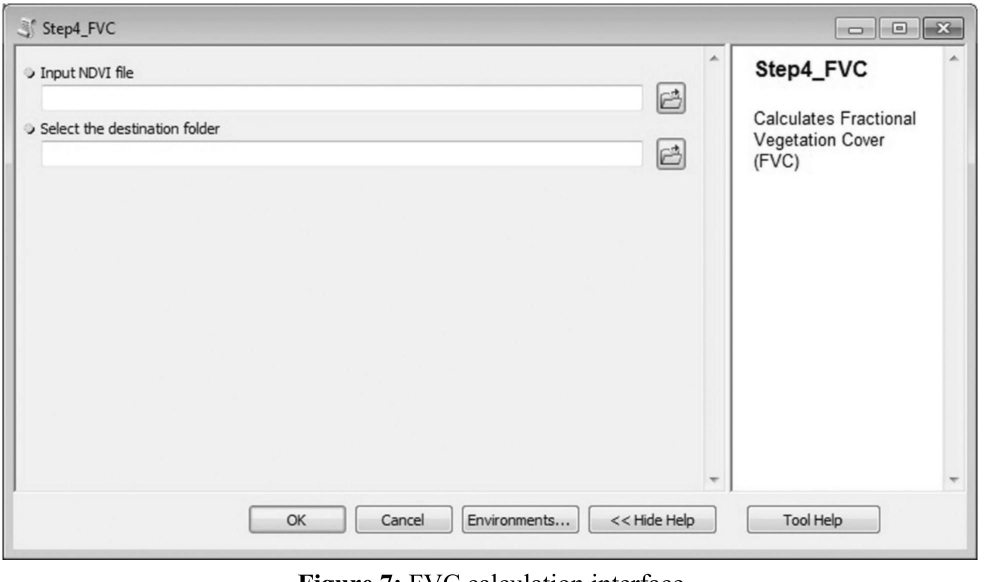


**Figure 7:** FVC calculation interface

The emissivity calculation interface is illustrated in Figure 8 below. This step requires only two parameters: 1- FVC file, and 2- Band 4 reflectance file.

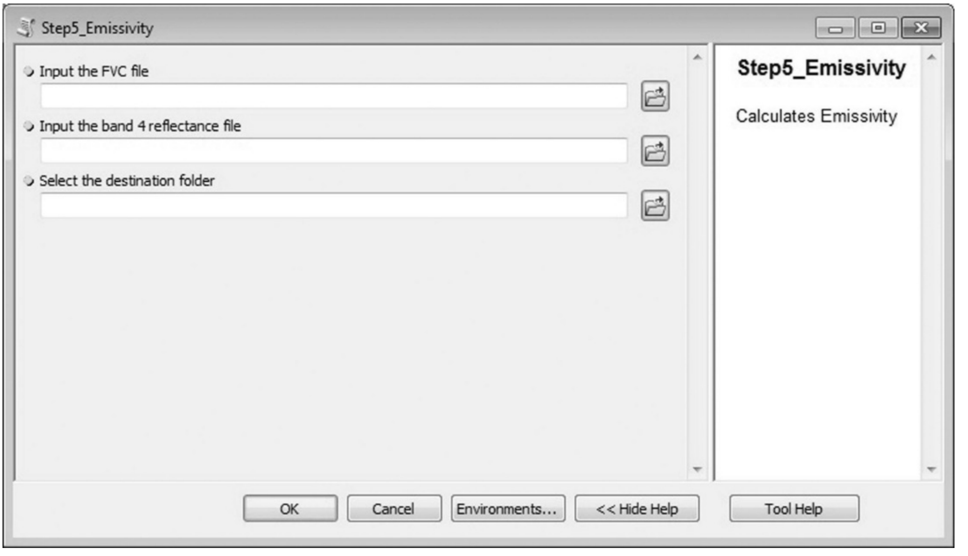


**Figure 8:** Emissivity calculation interface

The thermal radiance at sensor level (Lsen) calculation step requires five parameters: emissivity file, band 10 radiance file, down-welling atmospheric value, atmospheric transmission value, and up-welling atmospheric value, which can be obtained from Atmospheric Correction Parameter Calculator (ACPC) webpage (ACPC, 2016). The interface is shown in Figure 9 below.

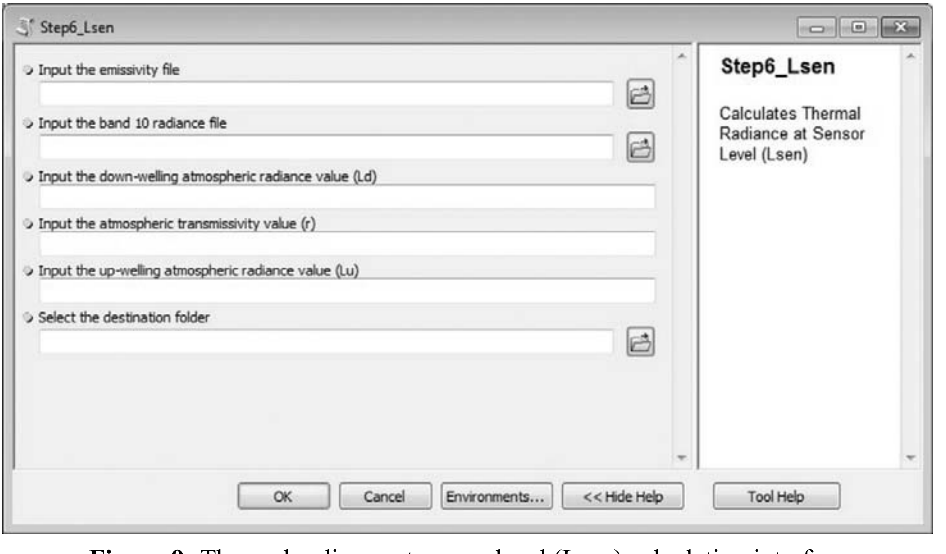


**Figure 9:** Thermal radiance at sensor level (Lsen) calculation interface

The final LST calculation interface requires emissivity file, the thermal radiance at sensor level file (Lsen), down-welling atmospheric radiance value, atmospheric transmission value, and up-welling atmospheric radiance value. The final LST calculation interface is seen in Figure 10 below.

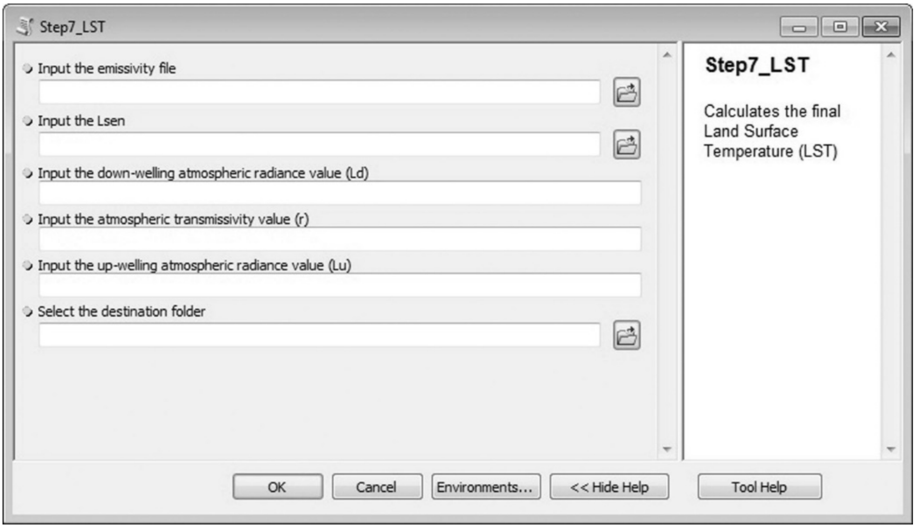


**Figure 10:** The final LST retrieval interface

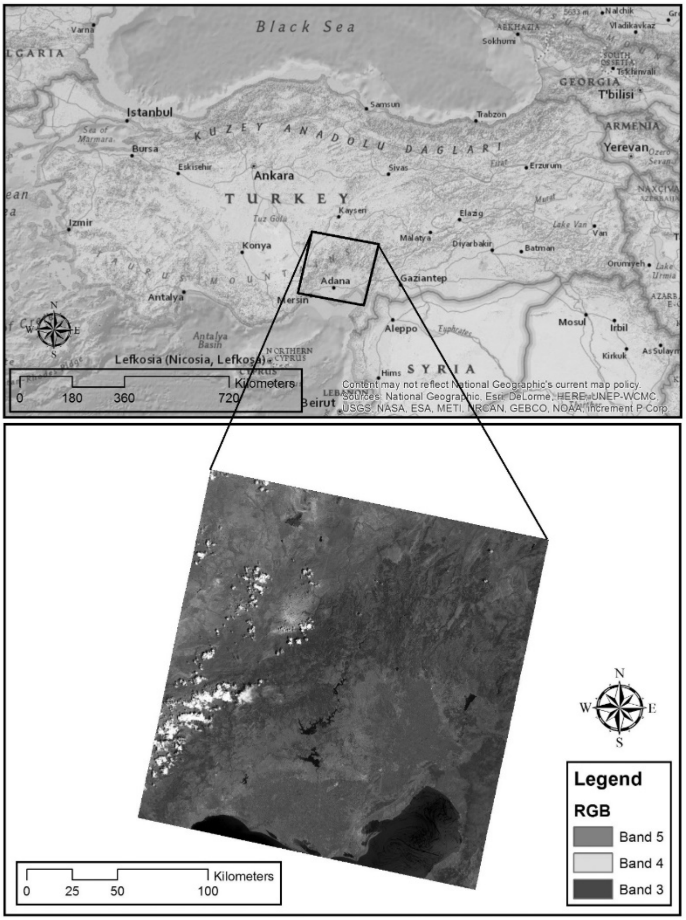


**Figure 11:** The sample Landsat 8 scene used in the demonstration

**Software Demonstration**

In order to demonstrate the LST Calculator toolbox, Adana, the fifth-largest city in Turkey has been selected as the study area as shown in Figure 11 above. Adana has witnessed a rapid development to become a metropolitan area and lies in the hearth of Cukurova which covers the cities of Adana, Mersin, Osmaniye, and Hatay. The region contains large flat fertile land that is regarded as one of the most productive areas of the world.

A Landsat 8 scene (path/row: 175/34), acquired on June 28 2014, was downloaded from Global Land Cover Facility website (GLCF, 2016). All the bands downloaded were resampled to 30m at GLCF except for panchromatic band that was distributed with 15m spatial resolution. The sample files and parameters used for demonstration are listed in Table 2 and Table 3 below.

**Table 2:** The sample files employed to calculate LST

| File Name | Data Type | File Dimension (Row x Column) | Description |
|---|---|---|---|
| Band 4 | TIF File | 7591 x 7741 | Landsat 8 RED Band |
| Band 5 | TIF File | 7591 x 7741 | Landsat 8 NIR Band |
| Band 10 | TIF File | 7591 x 7741 | Landsat 8 TIR Band |

**Table 3:** The parameters used for the sample files

| Parameter Name | Value |
|---|---|
| Atmospheric Transmissivity | 0.79 |
| Up-welling Atmospheric Radiance | 1.80 |
| Down-welling Atmospheric Radiance | 3.01 |
| Radiance multiplicative scaling factor for band 10 | $3.342 \times 10^{-4}$ |
| Radiance additive scaling factor for band 10 | 0.1 |
| Reflectance multiplicative scaling factor for band 4 | $2.0 \times 10^{-5}$ |
| Reflectance additive scaling factor for band 4 | -0.1 |
| Reflectance multiplicative scaling factor for band 5 | $2.0 \times 10^{-5}$ |
| Reflectance additive scaling factor for band 5 | -0.1 |

The final spatial distribution of LST map was illustrated in Figure 12. The minimum and maximum temperatures of the scene were computed as -130 ºC and 38 ºC. As predicted, high temperatures were retrieved within dense urban areas (ranging from 31 to 38 ºC) while extremely cold temperatures were calculated for the cloud cover (from -130 to -3 ºC). If we exclude cloud cover, the lowest temperatures belong to water area ranging from 3.5 to 18 ºC, and forested areas have temperatures ranging from 23 to 30 ºC as shown in Figure 12 below.

## DISCUSSION AND CONCLUSIONS

In this study, a Python toolbox was developed to retrieve land surface temperature from Landsat 8 imagery. This software can be an invaluable tool for those who are interested in thermal environment of earth's surface. This tool employs Radiative Transfer Equation algorithm for Landsat 8 and detailed information regarding the algorithm can be found in Skokovic *et al.*'s (2014) and Sobrino *et al.*'s (2008).

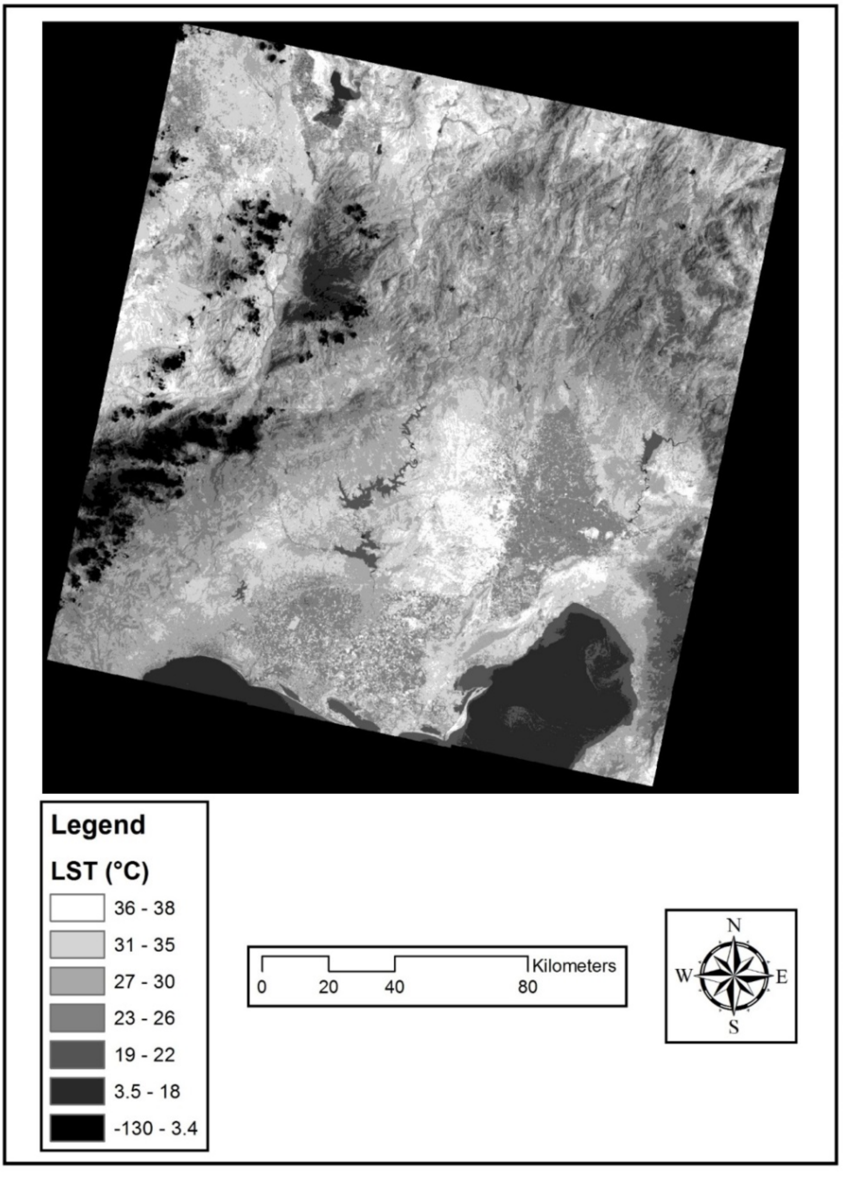


**Figure 12:** The spatial distribution pattern of land surface temperature

Furthermore, some atmospheric parameters are required prior to the calculation such as atmospheric transmissivity, up-welling and down-welling atmospheric radiances, which are essential to the retrieval of LST. These atmospheric parameters can be obtained from ACPC webpage (ACPC, 2016).

## REFERENCES

Abrams, M. (2000). The Advanced Spaceborne Thermal Emission and Reflection Radiometer (ASTER): Data products for the high spatial resolution imager on NASA's terra platform, International Journal of Remote Sensing, 21, (5), 847–859.

Abrams, M., Hook, S., & Ramachandran, B. (2008), ASTER user handbook: Version 2,Jet Propulsion Laboratory, Pasadena, CA, USA.
Beck, A., Anderson, G. P., Acharya, P. K., Chetwynd, J. H., Bernstein, L. S., Shettle, E. P., Matthew, M. W., & Adler-Golden, S. M. (1999). MODTRAN4 User's Manual, Hanscom AFB, MA: Air Force Res. Lab.
Cristóbal, J., Jiménez-Muñoz, J. C., Sobrino, J. A., Ninyerola, M. & Pons, X. (2009). Improvements in land surface temperature retrieval from the Landsat series thermal band using water vapor and air temperature, Journal of Geophysics Research, 114(D08), 103, Apr.
Gillespie, A., Rokugawa, S., Matsunaga, T., Cothern, J. S., Hook, S., & Kahle, A. B. (1998) A temperature and emissivity separation algorithm for Advanced Spaceborne Thermal Emission and Reflection Radiometer (ASTER) images, IEEE Transactions on Geosciences and Remote Sensing, 36(4), 1113–1126, Jul.
Gustafson, W. T. Gillespie, A. R., & Yamada, G. J. (2006). Revisions to the ASTER temperature/emissivity separation algorithm, in Proceedings Recent Advances in Quantitative Remote Sensing, Valencia, Spain, Sep. 25–29, 770–775.
Jiménez-Muñoz, J. C., & Sobrino, J. A. (2003). A generalized single-channel method for retrieving land surface temperature from remote sensing data, Journal of Geophysical Research, 108(D22), 4688, Nov.
Jimenez-Munoz, J. C., & Sobrino, J. A. (2007). Feasibility of retrieving land-surface temperature from ASTER TIR bands using two-channel algorithms: A case study of agricultural areas, IEEE Geoscience and Remote Sensing Letters, 4(1), 60–64, Jan.
Jimenez-Munoz, J. C., Sobrino, J. A., Gillespie, A., Sabol, D., & Gustafson, W. T. (2006). Improved land surface emissivities over agricultural areas using ASTER NDVI, Remote Sensing of Environment, 103(4), 474–487, Aug.
Jiménez-Muñoz, J. C., Cristóbal, J., Sobrino, J. A., Sòria, G., Ninyerola, M., & Pons, X. (2009). Revision of the single-channel algorithm for land surface temperature retrieval from Landsat thermal-infrared data, IEEE Transactions on Geosciences and Remote Sensing, 47(1), 339–349, Jan.
Jimenez-Munoz, J. C., Sobrino, J. A., Skokovic, D., Mattar, C., & Cristobal, J. (2014). Land Surface Temperature Retrieval Methods From Landsat 8 Thermal Infrared Sensor Data, IEEE Geoscience and Remote Sensing Letters 11, 10 Oct. 1840-1843.
Landsat 8 Data Users Handbook (2016). Department of the Interior US Geological Survey, Version 2.0, March 29.
Oguz, H. (2013). LST Calculator: A Program Retrieving Land Surface Temperature from Landsat TM/ETM+ Imagery, Environmental Engineering and Management Journal. 12(3), 549-555.
Oguz, H. (2015). A Software Tool for Retrieving Land Surface Temperature from Aster Imagery, Journal of Agricultural Sciences. 21, 471-482.
Skokovic D., Sobrino, J. A., Jimenez-Munoz, J. C., Soria, G., Julien, Y., Mattar, C., & Cristobal, J. (2014)
Calibration and Validation of land surface temperature for Landsat 8 - TIRS sensor, European Space Agency Documents.
Sobrino, J. A., Jiménez-Muñoz, J. C., Sòria, G., Romaguera, M., Guanter, L., Moreno, J., Plaza, A., & Martínez, P. (2008). Land Surface Emissivity Retrieval From Different VNIR and TIR Sensors, IEEE Transactions on Geoscience and Remote Sensing, 46(2), 316-327.
Sobrino, J. A., Jiménez-Muñoz, J. C., Balick, L., Gillespie, A., Sabol, D., & Gustafson, W. T. (2007) Accuracy of ASTER level-2 thermal-infrared standard products of an

agricultural area in Spain, Remote Sensing of Environment, 106(2), 146–153, Jan.
Sobrino, J. A., & Raissouni, N. (2000). Toward Remote Sensing Methods for Land Cover Dynamic Monitoring: Application to Morocco. International Journal of Remote Sensing 21, 353–66.
URL: ACPC (2016). http://atmcorr.gsfc.nasa.gov/ (accessed December 21, 2015).
URL: GLCF (2016) http://glcf.umiacs.umd.edu/ (accessed September 20, 2015).
Valor, E., & Caselles, V. (1996). Mapping Land Surface Emissivity from NDVI: Application to European, African, and South American Areas. Remote Sensing of Environment 57, 167–84.
Van de Griend, A. A., & Owe, M. (1993). On the Relationship between Thermal Emissivity and the Normalized Difference Vegetation Index for Natural Surfaces. International Journal of Remote Sensing 14, 1119–31.
Xiao, R., Ouyang, Z., Zheng, H., Li, W., Schienke, E.W., & Wang, X. (2007). Spatial pattern of impervious surfaces and their impacts on land surface temperature in Beijing, China. Journal of Environmental Sciences-China, 19, 250-256.
Yu, X., Guo, X., & Wu, Z. (2014) Land Surface Temperature Retrieval from Landsat 8 TIRS—Comparison between Radiative Transfer Equation-Based Method, Split Window Algorithm and Single Channel Method, Remote Sensing, 6, 9829--9852.